Electronic Supplementary Material (ESI) for Inorganic Chemistry Frontiers.
This journal is © the Partner Organisations 2022

Rapid Electron/Ion Transport in CNT/$LiTi_2(PO_4)_3$@C-N Electrodes for Aqueous Lithium-ion Batteries with High Stability, Flexibility and Safety

Jun Lin,[a] Zhigang Zhang,[a] Fangfang Xue,[a] Deng Long,[a] Qiuhong Li*[a]

* Pen-Tung Sah Institute of Micro-Nano Science and Technology, Xiamen University, Xiamen, 361005, PR China.

* Corresponding authors.

E-mail addresses: liqiuhong@xmu.edu.cn

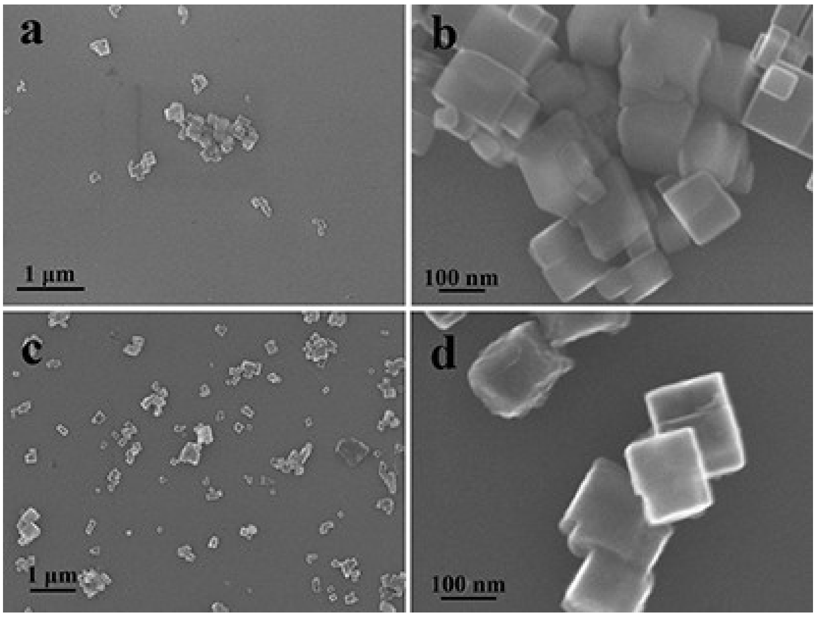

Fig. S1 SEM images of LTP (a, b) and LTP@C-N nanoparticles (c, d).

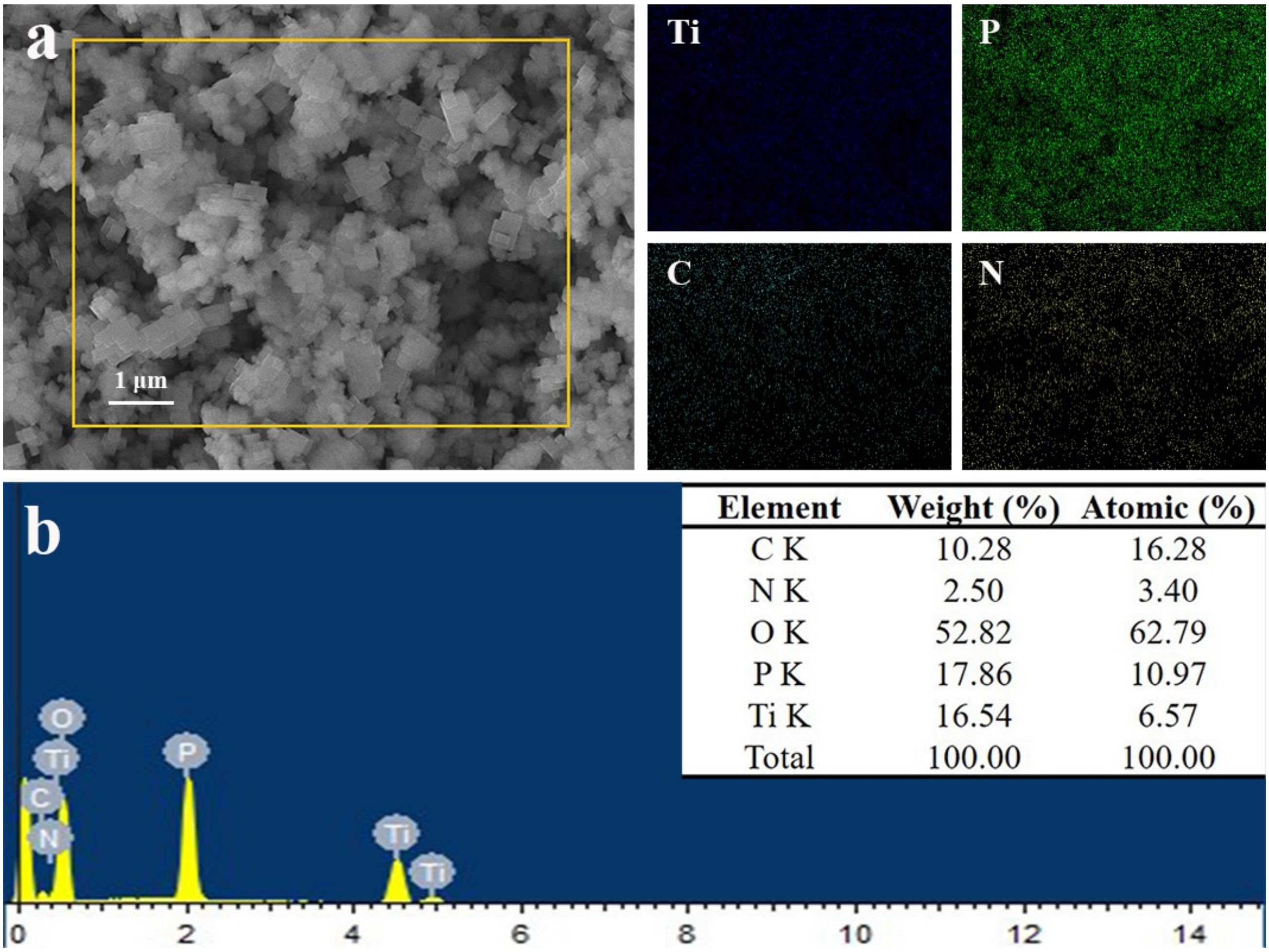

Fig. S2 (a) SEM image and corresponding element mapping images of Ti, P, C and N. (b) EDS spectrum of the LTP@C-N nanoparticles.

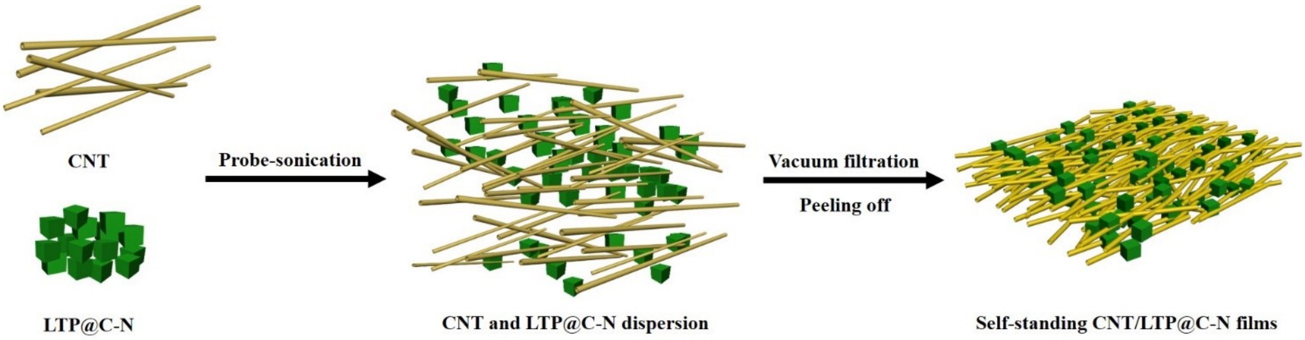

Fig. S3 Schematic illustration of the self-standing CNT/LTP@C-N films' preparation process.

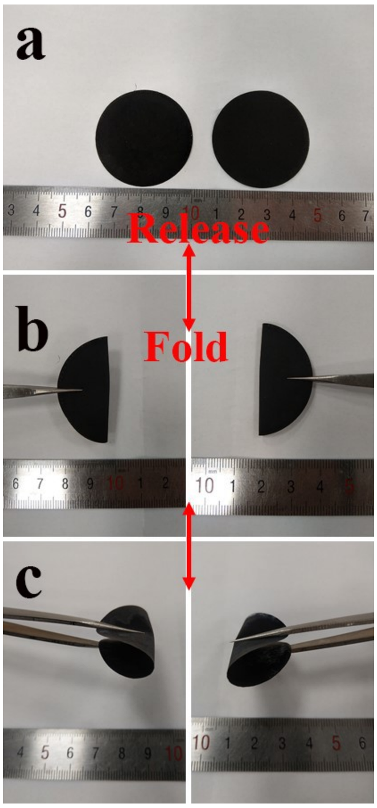

Fig. S4 Images of the CNT/LTP@C-N films before and after bending and folding.

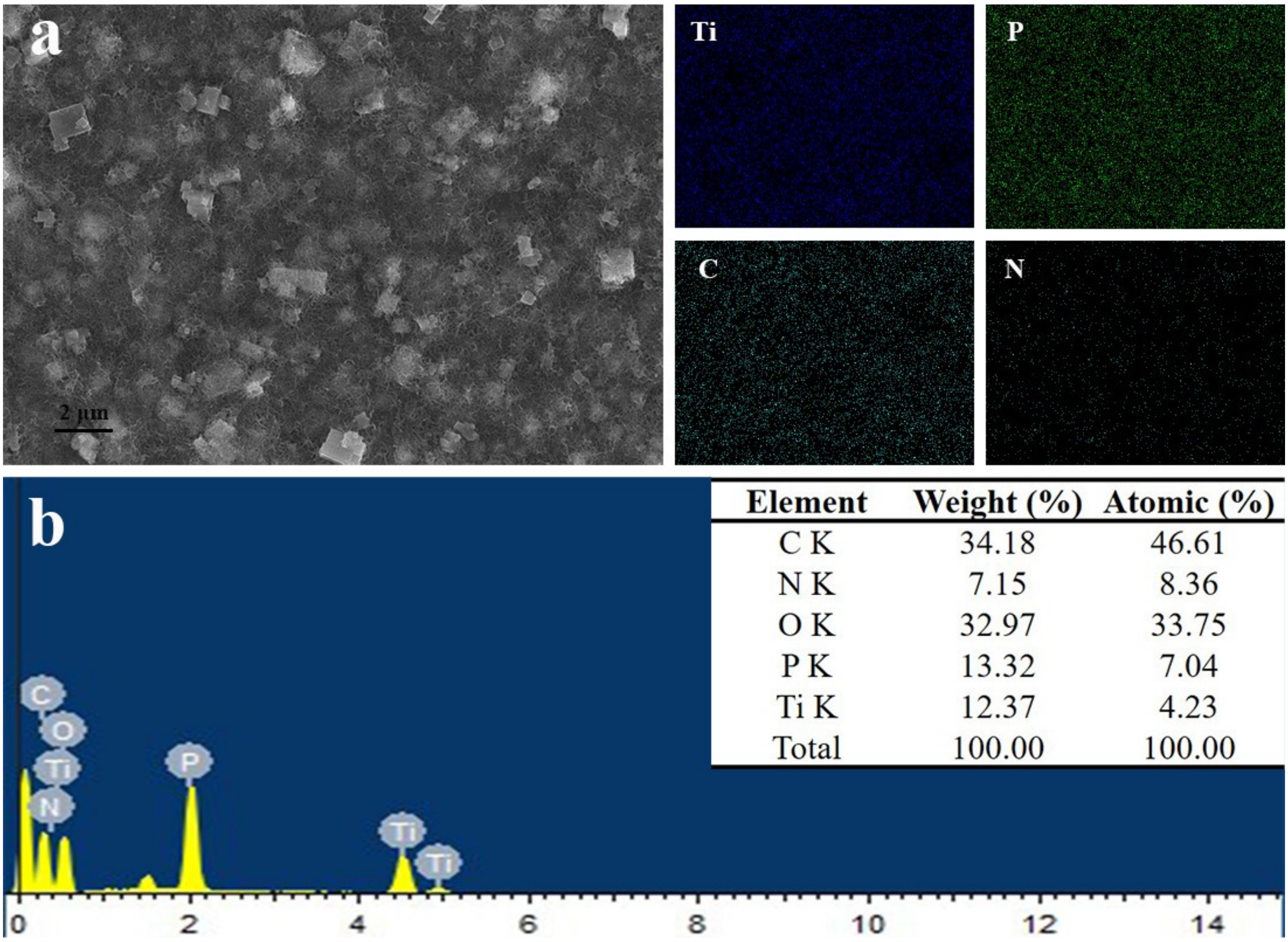

Element	Weight (%)	Atomic (%)
C K	34.18	46.61
N K	7.15	8.36
O K	32.97	33.75
P K	13.32	7.04
Ti K	12.37	4.23
Total	100.00	100.00

Fig. S5 (a) SEM image and corresponding element mapping images of CNT/LTP@C-N film from a sectional view. (b) EDS spectrum of CNT/LTP@C-N sample. The LTP@C-N particles uniformly distribute across the conductive and intertwined CNT network. Across the CNT/LTP@C-N film, Ti, P, C and N elements distribute evenly.

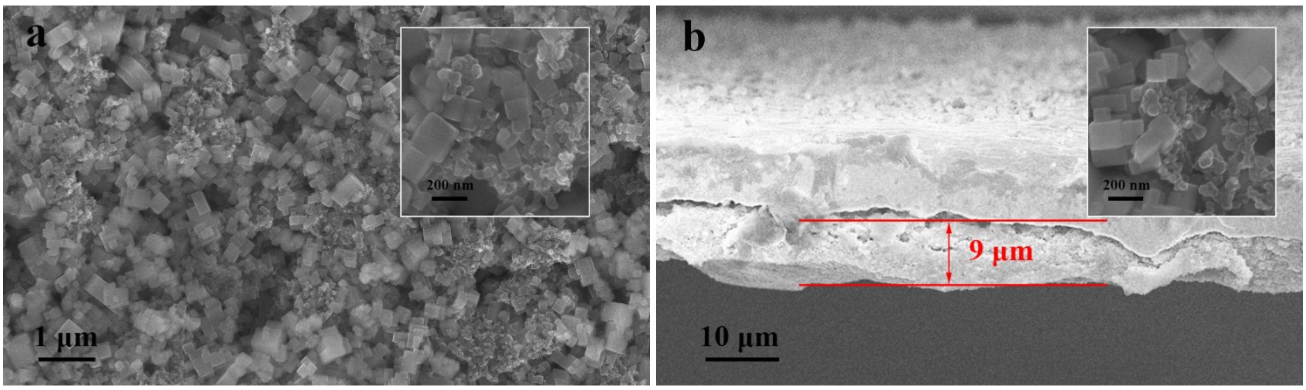

Fig. S6 (a) Top-view and (b) side-view FESEM images of the LTP electrode prepared by a conventional slurry coating method onto Cu foil. The insets in (a, b) are the enlarged region of the corresponding areas.

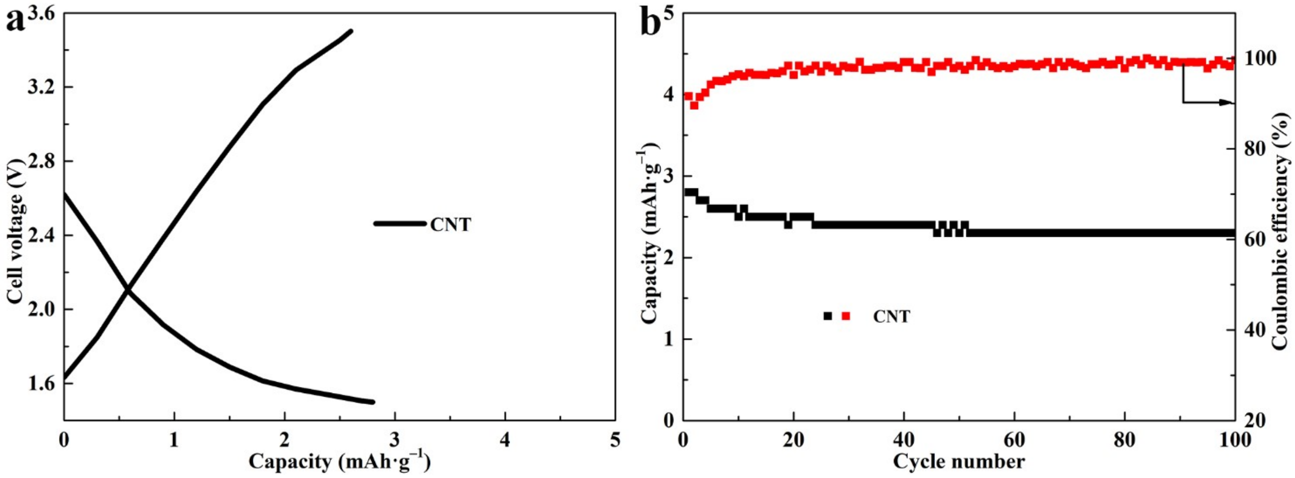

Fig. S7 (a) Charge/discharge profiles of CNT at 1 C (1 C=140 mAg^{-1}). (b) The cycle performance of CNT at 1 C in organic electrolyte.

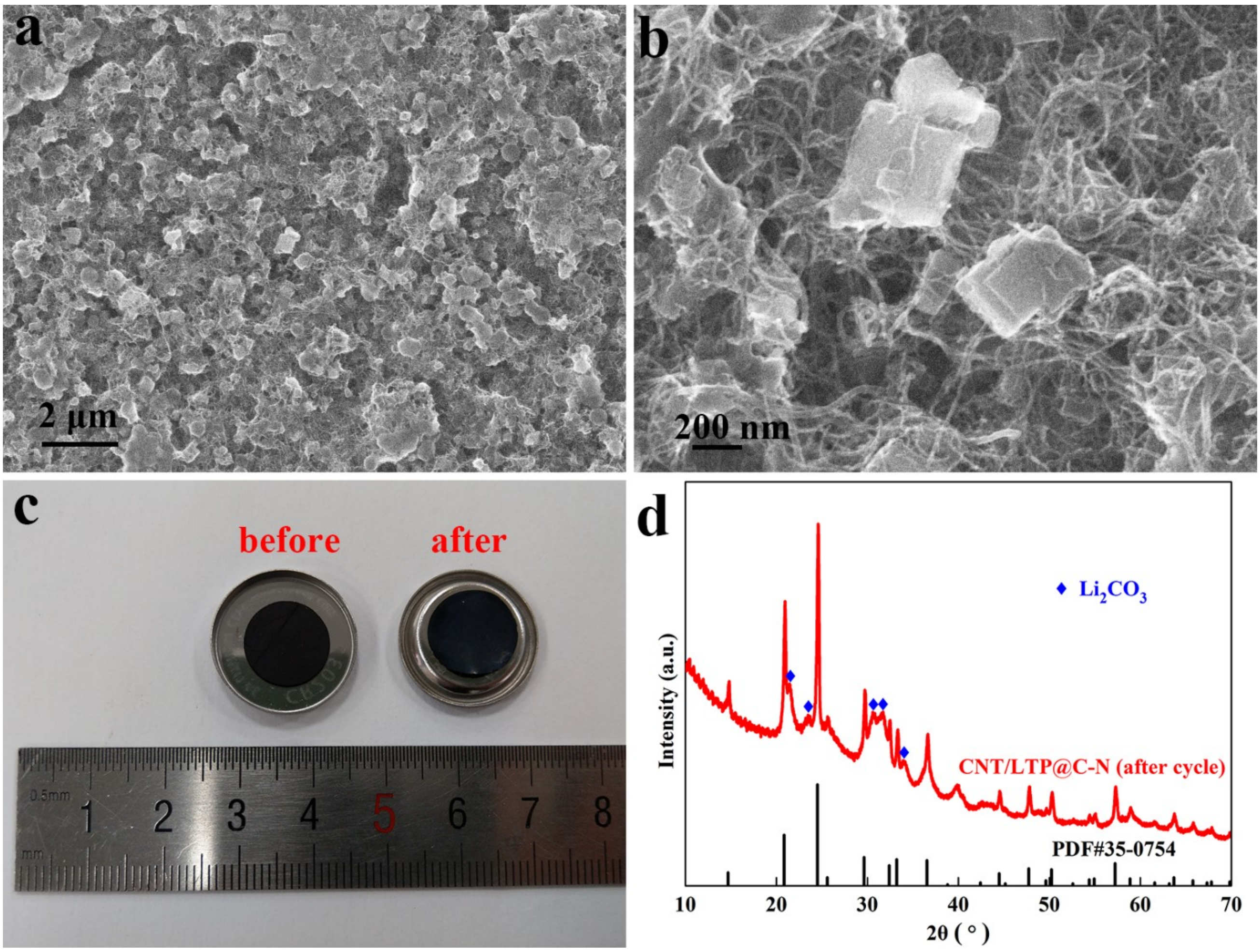

Fig. S8 The morphology and phase of the CNT/LTP@C-N free-standing electrode after cycles: (a) low-magnification and (b) high-magnification SEM images. (c) Photograph, showing good structural integrity. (d) XRD pattern.

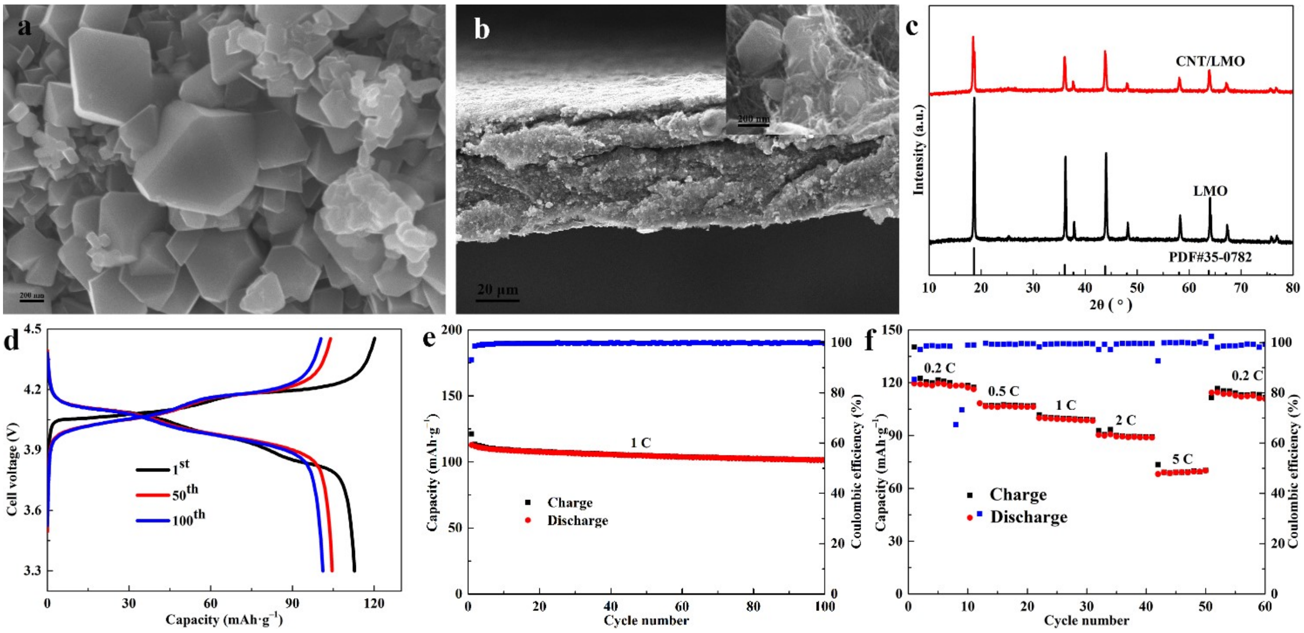

Fig. S9 (a, b) SEM images of the as-prepared LMO and CNT/LMO samples. (c) XRD pattern. (d) Charge/discharge profiles of CNT/LMO cathode at 1 C (1 C=148 mAg^{-1}). (e) The cycle performance of CNT/LMO at 1 C. (f) Rate performance in organic electrolyte.

Table S1. The data of LTP, LTP@C-N and CNT/LTP@C-N based on the equivalent circuit.

sample	Rs(Ω)	Rct(Ω)	RSEI(Ω)
LTP	4.922	286.6	86.89
LTP@C-N	6.004	119.1	24.43
CNT/LTP@C-N	3.95	32.32	/

Table S2. Comparison of the electrochemical performance of LTP-based anode materials for LIBs.

LTP anode materials	**Rate Capability**		**Cycle performance**	
	C-rates	Specific Capacity (mAh/g)	Cycle life at different C-rate	Capacity retention
rGO-LTP hybrid[1]	1 C	123	100 cycles @10 C	92 %
	50 C	83		
Sn-doped $LiTi_2(PO_4)_3$/C nanofibers[2]	100 mA g^{-1}	111	/	/
	2 A g^{-1}	102		
$LiTi_2(PO_4)_3$@N-C Composite[3]	20 C	120	1000 cycles@10 C	89.5 %
	50 C	87		
$LiTi_2(PO_4)_3$/C[4]	1 C	125.6	1000 cycles@5 C	94.4 %
	10 C	92.5	1000 cycles@20 C	80.4 %
$LiTi_2(PO_4)_3$/C[5]	0.1 C	133.8	500 cycles@5 C	97.7 %
	100 C	20		
$LiTi_2(PO_4)_{2.88}F_{0.12}$[6]	10 C	107	1000 cycles@10 C	87.8 %
	40 C	90		
$LiTi_2(PO_4)_3$/C[7]	1 C	114	1000 cycles@10 C	90 %
	20 C	84		
$LiTi_2(PO_4)_3$/C[8]	0.5 C	109.8	2000 cycles@10 C	85 %
	20 C	84.4		
$LiTi_2(PO_4)_3$/CNT[9]	0.05 C	133.8	200 cycles@0.1 C	96.2 %
CNT/LTP@C-N (This work)	1 C	143	200 cycles@1 C	93.4 %
	30 C	85	1500 cycles@5 C	87.3 %

Table S3. Comparison of the electrochemical performance of the state-of-the-art aqueous lithium-ion batteries.

LTP anode materials	**Rate Capability**		**Cycle performance**	
	C-rates	Specific Capacity (mAh/g)	Cycle life at different C-rate	Capacity retention
VO_2(B)/C//$LiMn_2O_4$[10]	/	/	25 cycles @0.69 mA cm^{-2}	Failed
$LiTi_2(PO_4)_3$//$LiFePO_4$[11]	1 C	55	1000 cycles @1 C	90 %
Mo_6S_8//$LiMn_2O_4$[12]	0.15 C	40	1000 cycles @4.5 C	72 %
	4.5 C	30		
Mo_6S_8//$LiNi_{0.5}Mn_{1.5}O_4$[13]	0.15 C	30	400 cycles @5 C	70 %
	4.5 C	17		
Mo_6S_8//$LiCoO_2$[14]	0.5 C	60	1000 cycles @2.5 C	87 %
	2.5 C	38		
$LiFePO_4$//$LiFePO_4$[15]	0.5 C	116	500 cycles @1.1 C	80 %
	5 C	50		
LiV_3O_8//$LiMn_2O_4$[16]	0.1 A g^{-1}	32	500 cycles @0.5 A g^{-1}	80 %
$LiVPO_4F$/$LiVPO_4F$[17]	2 C	58.1	4000 cycles @20 C	87 %
	60 C	40.8		
$LiTi_2(PO_4)_3$/$LiCoO_2$[18]	1 C	130.3	2000 cycles @1 C	86 %
	50 C	112.1		
$LiTi_2(PO_4)_3$/$LiMn_2O_4$[19]	1 C	105	120 cycles @1 C	80.6 %
	10 C	89	120 cycles @10 C	97 %
$LiTi_2(PO_4)_3$/$LiMn_2O_4$[3]	1 C	123	100 cycles @0.22 C	91.2 %
	10 C	103	400 cycles @1.08 C	90.4 %
CNT/LTP@C-N//$LiMn_2O_4$ (This work)	1 C	126.5	200 cycles @1 C	96.3 %
	15 C	57	1000 cycles @3 C	70.2 %

References

1 C.H. Lim, A.G. Kannan, H.W. Lee, D.K. Kim, A high power density electrode with ultralow carbon via direct growth of particles on graphene sheets, J. Mater. Chem. A, 2013, **1**, 6183-6190.

2 L. Liu, T. Song, H. Han, H. Park, J. Xiang, Z. Liu, Y. Feng, U. Paik, Electrospun Sn-doped $LiTi_2(PO_4)_3$/C nanofibers for ultra-fast charging and discharging, J. Mater. Chem. A, 2015, **3**, 10395-10402.

3 D. Sun, X. Xue, Y. Tang, Y. Jing, B. Huang, Y. Ren, Y. Yao, H. Wang, G. Cao, High-Rate $LiTi_2(PO_4)_3$@N-C Composite via Bi-nitrogen Sources Doping, ACS Appl. Mater. Interfaces, 2015, **7**, 28337-28345.

4 J. Sun, Y. Sun, L. Gai, H. Jiang, Y. Tian, Carbon-coated mesoporous $LiTi_2(PO_4)_3$ nanocrystals with superior performance for lithium-ion batteries, Electrochim. Acta, 2016, **200**, 66-74.

5 S. Yu, H. Tempel, R. Schierholz, O. Aslanbas, X. Gao, J. Mertens, L.G.J. de Haart, H. Kungl, R.A. Eichel, $LiTi_2(PO_4)_3$/C Anode Material with a Spindle-Like Morphology for Batteries with High Rate Capability and Improved Cycle Life, ChemElectroChem, 2016, **3**, 1157-1169.

6 H. Wang, H. Zhang, Y. Cheng, K. Feng, X. Li, H. Zhang, Rational design and synthesis of $LiTi_2(PO_4)_{3-x}F_x$ anode materials for high-performance aqueous lithium ion batteries, J. Mater. Chem. A, 2017, **5**, 593-599.

7 W. Sun, J. Liu, X. Liu, X. Fan, K. Zhou, X. Wei, Bimolecular-induced hierarchical nanoporous $LiTi_2(PO_4)_3$/C with superior high-rate and cycling performance, ChemComm, 2017, **53**, 8703-8706.

8 M. Li, L. Liu, N. Zhang, S. Nie, Q. Leng, J. Xie, Y. Ouyang, J. Xia, Y. Zhang, F. Cheng, X. Wang, Mesoporous $LiTi_2(PO_4)_3$/C composite with trace amount of carbon as high-performance electrode materials for lithium ion batteries, J. Alloys Compd., 2018, **749**, 1019-1027.

9 S. Yu, Q. Xu, C.L. Tsai, M. Hoffmeyer, X. Lu, Q. Ma, H. Tempel, H. Kungl, H.D. Wiemhoefer, R.A. Eichel, Flexible All-Solid-State Li-Ion Battery Manufacturable in Ambient Atmosphere, ACS Appl. Mater. Interfaces, 2020, **12**, 37067-37078.

10 W. Li, J.R. Dahn, D.S. Wainwright, Rechargeable lithium batteries with aqueous electrolytes, Science, 1994, **264,** 1115-1118.

11 J. Y. Luo, W. J. Cui, P. He, Y. Y. Xia, Raising the cycling stability of aqueous lithium-ion batteries by eliminating oxygen in the electrolyte, Nat. Chem., 2010, **2**, 760-765.

12 L. Suo, O. Borodin, T. Gao, M. Olguin, J. Ho, X. Fan, C. Luo, C. Wang, K. Xu, "Water-in-salt" electrolyte enables high-voltage aqueous lithium-ion chemistries, Science, 2015, **350**, 938-943.

13 F. Wang, L. Suo, Y. Liang, C. Yang, F. Han, T. Gao, W. Sun, C. Wang, Spinel $LiNi_{0.5}Mn_{1.5}O_4$ Cathode for High-Energy Aqueous Lithium-Ion Batteries, Adv. Energy Mater., 2017, **7**, 1600922.

14 F. Wang, Y. Lin, L. Suo, X. Fan, T. Gao, C. Yang, F. Han, Y. Qi, K. Xu, C. Wang, Stabilizing high voltage $LiCoO_2$ cathode in aqueous electrolyte with interphase-forming additive, Energy Environ. Sci., 2016, **9**, 3666-3673.

15 D. Gordon, M.Y. Wu, A. Ramanujapuram, J. Benson, J.T. Lee, A. Magasinski, N. Nitta, C. Huang, G. Yushin, Enhancing Cycle Stability of Lithium Iron Phosphate in Aqueous Electrolytes by Increasing Electrolyte Molarity, Adv. Energy Mater., 2016, **6**, 1501805.

16 Z. Liu, H. Li, M. Zhu, Y. Huang, Z. Tang, Z. Pei, Z. Wang, Z. Shi, J. Liu, Y. Huang, C. Zhi, Towards wearable electronic devices: A quasi-solid-state aqueous lithium-ion battery with outstanding stability, flexibility, safety and breathability, Nano Energy, 2018, **44**, 164-173.

17 C. Yang, X. Ji, X. Fan, T. Gao, L. Suo, F. Wang, W. Sun, J. Chen, L. Chen, F. Han, L. Miao, K. Xu, K. Gerasopoulos, C. Wang, Flexible Aqueous Li-Ion Battery with High Energy and Power Densities, Adv. Mater., 2017, **29**, 1701972.

18 L. Xue, Q. Zhang, X. Zhu, L. Gu, J. Yue, Q. Xia, T. Xing, T. Chen, Y. Yao, H. Xia, 3D $LiCoO_2$ nanosheets assembled nanorod arrays via confined dissolution-recrystallization for advanced aqueous lithium-ion batteries,

Nano Energy, 2019, **56**, 463-472.
19 Z. Liu, X. Qin, H. Xu, G. Chen, One-pot synthesis of carbon-coated nanosized $LiTi_2(PO_4)_3$ as anode materials for aqueous lithium ion batteries, J. Power Sour., 2015, **293**, 562-569.